Density Stratification, Turbulence, but How Much Mixing?

G.N. Ivey,[1] K.B. Winters,[2] and J.R. Koseff[3]

[1]School of Environmental Systems Engineering, University of Western Australia, Nedlands, Australia 6008; email: ivey@sese.uwa.edu.au

[2]Scripps Institution of Oceanography, La Jolla, California 92307

[3]Department of Civil and Environmental Engineering, Stanford University, Stanford, California 94305-4020

Annu. Rev. Fluid Mech. 2008. 40:169–84

The *Annual Review of Fluid Mechanics* is online at fluid.annualreviews.org

This article's doi:
10.1146/annurev.fluid.39.050905.110314

0066-4189/08/0115-0169$20.00

Key Words

internal waves, ocean dynamics, estuaries, lakes

Abstract

We examine observations of turbulence in the geophysical environment, primarily from oceans but also from lakes, in light of theory and experimental studies undertaken in the laboratory and with numerical simulation. Our focus is on turbulence in density-stratified environments and on the irreversible fluxes of tracers that actively contribute to the density field. Our understanding to date has come from focusing on physical problems characterized by high Reynolds number flows with no spatial or temporal variability, and we examine the applicability of these results to the natural or geophysical-scale problems. We conclude that our sampling and interpretation of the results remain a first-order issue, and despite decades of ship-based observations we do not begin to approach a reliable sampling of the overall turbulent structure of the ocean interior.

INTRODUCTION

In fields as diverse as oceanography, atmospheric physics, and engineering, the quantification of the vertical flux of active tracers, passive tracers, and momentum due to small-scale turbulent processes represents an ongoing challenge. In the ocean thermocline region, direct estimates of vertical fluxes are generally an order of magnitude smaller than those required to close bulk estimates, suggesting that the majority of the mixing must occur elsewhere, either at boundaries or in undersampled hot spots in the ocean interior at which mixing rates are considerably higher. Much of the mixing is thought to be associated with topographically complex boundary areas (e.g., Munk & Wunsch 1998, Wunsch & Ferrari 2004). Wunsch & Ferrari (2004) showed that a crucial unknown in global-scale energy budgets is the efficiency of energy transfer from tidal forcing to small-scale turbulent mixing. Questions regarding ocean energetics and mixing efficiency are especially important in efforts to calculate the ocean state under very different conditions than those existing today, for example, under climate-change scenarios. The issue arises both in the context of simple models of the natural environment as well as the need for quantitative descriptions in complex numerical models of the ocean and atmospheric circulation.

It is thus crucial to be able to describe small-scale mixing with high accuracy. Owing to computational constraints, numerical models of the ocean circulation have typical model resolution in the range of 1–10 m in the vertical scale. They therefore must employ subgrid-scale parameterizations to describe the consequence of subgrid-scale turbulent processes in terms of resolved scale motions. Although many closure schemes have been proposed, there is now a particular focus on the performance of these models in boundary and coastal regions (e.g., Durski et al. 2004). These important regions of the ocean are particularly challenging to model owing to topographical complexity, strong density stratifications, intense current fields, and the rapid changes (compared with the deep ocean) in these quantities that can occur in time as well as in space, both vertically and horizontally, in the density and velocity fields. Durski et al. (2004), for example, compared different closure schemes and showed they can produce significantly different solutions in the coastal region. In confined water bodies such as estuaries and lakes, these issues become even more severe (e.g., Stacey et al. 1999).

So why is this specification of the vertical mixing so difficult? A fundamental problem is that the gravitationally influenced vertical component of the turbulent mixing is highly unsteady and inhomogeneous, which, in turn, leads to fundamental measurement and interpretation problems. In the ocean, a mix of essentially quiescent and patchy turbulent regions exists, and the turbulence intensity is highly variable even in the turbulent regions. In the time domain, turbulence intensity can vary from laminar to turbulent and back again, as illustrated nicely in the breaking internal wave images shown in **Figure 1**. How do we develop models that can describe these transitions in time and space that are ubiquitous in nature?

Most closure schemes in models are based around the idea of steady, homogeneous, and high Reynolds number flows. They typically describe mixing with an eddy diffusivity for density K_ρ computed from a knowledge of the local gradient Richardson

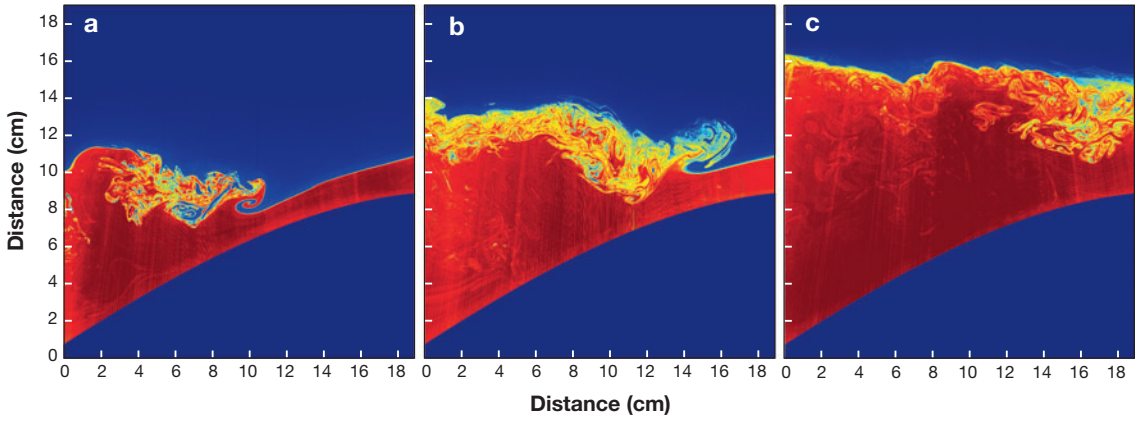

Figure 1

An example from a laboratory study of the evolution of a turbulent mixing event driven by the breaking of an internal wave on sloping bottom topography. The planar laser-induced fluorescence images show the background two-layer density field with an internal wave breaking at the interface. The temporal spacing between the three images (*a–c*) is $t/T = 0.10$, where the wave period is $T = 27$ s. Figure taken from Troy et al. 2006.

number *Ri*:

$$Ri = \frac{N^2}{S^2}, \tag{1}$$

where $N = (-gd\rho/dz/\rho)^{1/2}$ is the buoyancy frequency dependent on the local background density gradient $\rho(z)$, and $S = (dU/dz)$ is the vertical shear in the mean horizontal velocity $U(z)$. The quantities N and S are computed between adjacent horizontal layers, that is, on scales ranging from 1–10 m, depending on model vertical resolution. When $Ri > 0.25$, buoyancy suppresses turbulence, and transport must drop to values approaching the molecular limit. When $Ri < 0.25$, buoyancy is unable to suppress the turbulence, and the eddy diffusivity K_ρ is dependent on a function of *Ri* that must be determined (e.g., Durski et al. 2004). If much of the geophysical environment is characterized by either laminar or weakly turbulent regions, how well do these models work in the regime in which the turbulent diffusivity K_ρ varies between $\kappa \leq K_\rho \leq 100\kappa$, for example?

Our purpose is to examine observations of turbulence in the environment, primarily from oceans but also from lakes, in light of theory and experimental studies undertaken in the laboratory and in direct numerical simulation (DNS). The field is large, and we refer the reader to the recent reviews of related subjects by Riley & Lelong (2000), Staquet & Sommeria (2002), and Baumert et al. (2005). Our focus here is on turbulence in density-stratified environments and on the irreversible fluxes of tracers that actively contribute to the density field. We are particularly interested in those environments that are at the weaker end of the turbulent state, defined here as the effective diffusivities that are typically one or at most two orders of magnitude greater than molecular rates. This appears to be the state of many natural geophysical

flows, and interestingly, it is the range in which internal waves and turbulence coexist. As we discuss below, our present understanding has come from focusing on physical problems characterized by high Reynolds number flows with no spatial or temporal variability. The question here is how applicable are these results to the natural or geophysical-scale problems, and we examine this by reference to different physical scenarios.

APPROACHES AND METHODS

It is useful to examine current work in the context of some simple dimensionless numbers. Introducing velocity and length scales q and l that characterize the turbulent flow, and characterizing the ambient fluid with the density stratification N and the viscosity ν, we then arrive at a simple set of dimensionless parameters for stratified turbulence:

$$Fr_T = \frac{q}{Nl}, \quad \mathrm{Re}_T = \frac{ql}{\nu}, \quad \text{and} \quad I = \frac{\varepsilon}{\nu N^2}. \tag{2a}$$

All three parameters are commonly used, but by the Buckingham π theorem, only two are needed to characterize the problem providing one can write the turbulent kinetic energy dissipation rate as $\varepsilon = q^3/l$. The three parameters are thus not independent and are related by $Fr_T = (I/\mathrm{Re}_T)^{1/2}$ (Ivey & Imberger 1991). The first two parameters in Equation 2a are the turbulent Froude and Reynolds numbers, analogous in meaning to the mean flow equivalents. The third parameter, I, can be interpreted as the ratio of the destabilizing effects of turbulent stirring to the stabilizing effects resulting from the combined action of buoyancy and viscosity. Alternatively, one can interpret I as the ratio of the buoyancy time scale ($1/N$) to the time it takes for turbulent events to fully develop $(\varepsilon/\nu)^{1/2}$. If this ratio is large (high values of I), the turbulence is only weakly affected by buoyancy because it develops relatively rapidly.

Unlike many engineering flows, owing to variability in the mean or internal wave fields, turbulence in geophysical flows is intermittent, and we denote this time scale of variability as T. Furthermore, the turbulent fields are typically spatially inhomogeneous, and we characterize this by the scale L. One could introduce both lateral and vertical scales of variability here, but because we are interested in the vertical fluxes, we think of L as a vertical length scale. Thus two further dimensionless scales are required, for example,

$$\frac{l}{L} \quad \text{and} \quad \frac{(l/q)}{T}. \tag{2b}$$

Whether we are talking about laboratory, field, or numerical methods, the value and range of these five parameters are important for characterizing the turbulent mixing. We can conveniently divide approaches to turbulent mixing into two categories: indirect and direct measurements of the vertical flux.

Indirect measurements do not measure the vertical turbulent density flux $\overline{\rho' w'}$ (or equally buoyancy flux $\overline{b' w'}$); rather they typically measure a scalar turbulent quantity, such as ε or χ, the temperature variance dissipation rate, and then use models to infer the value of K_ρ. A commonly used indirect model (Osborn 1980) is based on the

turbulent kinetic energy equation

$$-\frac{1}{2}\frac{\partial \overline{u_i'^2}}{\partial t} - \frac{1}{2}\overline{u}_j\frac{\partial \overline{u_i'^2}}{\partial x_j} - \overline{u_i'u_j'}\frac{\partial \overline{u}_i}{\partial x_j} - \frac{\partial}{\partial x_j}\left(\overline{\frac{1}{2}u_j'u_i'u_i'} + \frac{1}{\overline{\rho}}\overline{u_j'p'} + \nu\overline{u_i'\frac{\partial u_i'}{\partial x_j}}\right) = b + \varepsilon. \quad (3)$$

If $l/L = 0$ and $(q/l)/T = 0$, then one can neglect unsteadiness, transport of turbulent kinetic energy by the mean flow, and all the divergence terms, and Equation 3 reduces to a simple balance between local shear production, buoyancy flux, and dissipation:

$$-\overline{u_i'u_j'}\frac{\partial \overline{u}_i}{\partial x_j} = b + \varepsilon. \quad (4)$$

Hence the vertical eddy diffusivity is

$$K_\rho = -\frac{b}{N^2} = \left(\frac{R_f}{1+R_f}\right)\frac{\varepsilon}{N^2} = \Gamma\frac{\varepsilon}{N^2}, \quad (5)$$

where the flux Richardson number R_f, a measure of the mixing efficiency, is defined from Equation 4 as

$$R_f = \frac{b}{-\overline{u'w'}\frac{\partial \overline{u}}{\partial z} - \overline{v'w'}\frac{\partial \overline{v}}{\partial z}}. \quad (6)$$

One must independently determine the flux Richardson number R_f, and, on the basis of laboratory experiments at the time, Osborn (1980) suggested $R_f \leq 0.17$ (and hence $\Gamma \leq 0.2$). Thus measurements of ε and N allow the determination of an upper bound for the diffusivity K_ρ from Equation 5. Note that the formulation in Equation 5 does not answer the following question: As the turbulence intensity decreases, when does the turbulent diffusivity K_ρ revert to its molecular value κ?

The second commonly used indirect model (Osborn & Cox 1972) is based on the temperature variance equation

$$\frac{\partial \overline{\theta'^2}}{\partial t} + \overline{u}_j\frac{\partial \overline{\theta'^2}}{\partial x_j} + 2\overline{u_j'\theta}\frac{\partial \bar{\theta}}{\partial x_j} - \frac{\partial}{\partial x_j}\left(\overline{u_j'\theta'^2} + \kappa\frac{\partial \overline{\theta'^2}}{\partial x_j}\right) = -2\kappa\overline{\left(\frac{\partial \theta'}{\partial x_j}\right)^2}. \quad (7)$$

Again if $l/L = 0$ and $(q/l)/T = 0$, then one can neglect unsteadiness, advection by the mean flow, and all the divergence terms, and Equation 8 simplifies to

$$2\overline{u_j'\theta}\frac{\partial \bar{\theta}}{\partial x_j} = -2\kappa\overline{\left(\frac{\partial \theta'}{\partial x_j}\right)^2} = \chi, \quad (8)$$

where χ is the rate of dissipation of temperature variance. Assuming further that the turbulence is isotropic at the smallest scales, that all mean and turbulent density gradients are taken in the normal direction n to the isothermal surfaces, and that the mean gradient is defined with respect to the sorted state of minimum potential energy (Winters & D'Asaro 1996), then from Equation 8 the eddy diffusivity for heat K_θ is

$$K_\theta = 3\kappa\frac{\overline{\left(\frac{\partial \theta'}{\partial n}\right)^2}}{\left(\frac{\partial \bar{\theta}}{\partial n}\right)^2}. \quad (9)$$

In the field, n is always assumed to be in the z direction (e.g., Sherman & Davis 1995). If temperature is the sole contributor to density, it is thus tempting to equate

K_θ in Equation 9 with K_ρ in Equation 5 and infer the unknown mixing efficiency R_f (e.g., Oakey 1982). However, apart from needing simultaneous and independent measurements of both the turbulent velocity and temperature signatures, the procedure requires that all the assumptions leading to Equation 5 and all the assumptions leading to Equation 9 are both satisfied at a point in the ocean.

Researchers have expended much effort in the laboratory and, more recently, in DNS to evaluate the effectiveness of models such as Equations 5 and 9. Laboratory experiments in density-stratified wind and water tunnels have been designed so they provide for steady forcing and homogenous turbulence conditions, enabling the extraction of long time series to estimate mixing (e.g., Itsweire et al. 1986, Keller & Van Atta 2000, Rohr et al. 1988, Stillinger et al. 1983). Other experiments have used closed control volumes to estimate mixing over finite times during a steadily forced experiment (e.g., Barry et al. 2001, Jackson & Rehmann 2003, Linden 1979). Similarly, investigators have undertaken DNS experiments in sheared and stratified flows (e.g., Briggs et al. 1998, Itsweire et al. 1993, Shih et al. 2005, Smyth et al. 2001). The Prandtl $Pr = \nu/\kappa$ ranges from 1 to 700 in these studies. In both the laboratory and the DNS experiments, the turbulent Reynolds number Re_T is of order 10^2, but with the DNS calculations, one has the advantage of being able to compute the dissipation ε without making any assumptions regarding the isotropy of the dissipation tensor (e.g., Itsweire et al. 1993). In the DNS studies, there is no change in background potential energy; rather one calculates mixing by forming instantaneous volumetric averages of $\overline{\rho' w'}$, and hence $K_\rho = (-\overline{\rho' w'}/(d\bar{\rho}/dz))$.

Whether one uses either the definition in Equation 6 or the more fundamental definition of $R_f = b/(b + \varepsilon)$ (Ivey & Imberger 1991, Rohr et al. 1984), there is clear consensus from the laboratory and DNS work that R_f is highly variable and changes with mechanism, the evolutionary stage of a turbulent event, and location in the domain (e.g., Barry et al. 2001, Shih et al. 2005, Smyth et al. 2001). For steady forcing, when $\varepsilon/\nu N^2 \to 1$, the mixing efficiency $R_f \to 0$ and $K_\rho \to \kappa$. At the other extreme, when $\varepsilon/\nu N^2 \to 10^5$, the mixing efficiency $R_f \to 0$ and $K_\rho \to 10^2\kappa$. Between these two extremes, when $\varepsilon/\nu N^2 \sim O(10^2)$, the mixing efficiency is maximal with $R_f \approx 0.25$ and $K_\rho \approx 10\kappa$.

From their DNS results, Shih et al. (2005) suggested the existence of three regimes of mixing: a molecular regime M, a transitional regime we denote here by T, and finally a fully energetic regime E. The transition from regime M to T occurs when $I = \varepsilon/\nu N^2 > 7$, whereas the transition from regime T to E occurs when $I = \varepsilon/\nu N^2 > 100$. **Figure 2** summarizes their results. Although fundamental, $\varepsilon/\nu N^2$ is a small-scale turbulent quantity and does not provide a means to parameterize diffusivities in terms of easily resolvable mean flow properties. Nevertheless, for both regimes T and E, Shih et al. (2005) showed that $\varepsilon/\nu N^2 \sim \mathrm{Re}_T/Ri$ (see their figure 12), and hence the functional relationship for K_ρ depends on both mean and turbulent flow properties. Their results are reproduced here in **Table 1**. These resulting predictions are not consistent with the predictions in Equation 5 or 9. For example, the canonical form of Equation 5 of $K_\rho = 0.2(\varepsilon/N^2)$ only appears valid in the narrow transitional regime T, where $7 < \varepsilon/\nu N^2 < 100$, and beyond this range this canonical value greatly overestimates the actual diffusivity.

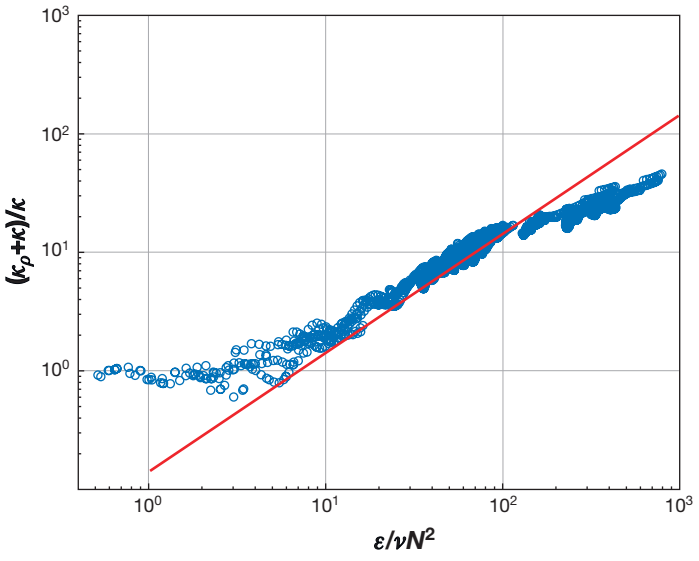

Figure 2

Eddy diffusivity K_ρ normalized by the molecular diffusivity κ as a function of $\varepsilon/\nu N^2$ from direct numerical simulation experiments. The prediction from Equation 5 with constant $\Gamma = 0.2$ is shown by the red line. Data taken from Shih et al. 2005.

APPLICATION TO THE FIELD

The above sections focus on the idealized theoretical frameworks in Equations 5 and 9 for treating mixing and the development of laboratory and numerical experiments. In this section, we consider the issues that arise when we try to apply these ideas to the field.

Mixing at Ocean Boundaries

As opposed to the indirect models in either Equation 5 or 9, there have been some attempts to measure $\overline{\rho' w'}$ directly. These few field measurements arise from vertical profiling instruments and have interpretation problems associated with the natural unsteadiness and patchiness in the environment. Although the instantaneous vertical density flux is measured, there are, for instance, almost as many examples of countergradient flux as there are of downgradient flux in these data (e.g., Lemckert et al. 2004, Saggio & Imberger 2001). As a consequence, almost all microstructure measurements in the ocean measure dissipation ε and rely on indirect methods to determine mixing.

Table 1 Mixing in continuously stratified fluids[a]

Regime	$\varepsilon/\nu N^2$ range	K_ρ^{Tot}	Re_T/Ri range	K_ρ^{Tot}
Molecular	$\varepsilon/\nu N^2 < 7$	κ	$Re_T/Ri < 150$	κ
Transitional	$7 < \varepsilon/\nu N^2 < 100$	$0.2\nu\left(\frac{\varepsilon}{\nu N^2}\right)^1$	$150 < Re_T/Ri < 1000$	$0.015\kappa\left(\frac{Re_T}{Ri}\right)^1$
Energetic	$\varepsilon/\nu N^2 > 100$	$2\nu\left(\frac{\varepsilon}{\nu N^2}\right)^{1/2}$	$Re_T/Ri > 1000$	$0.4\kappa\left(\frac{Re_T}{Ri}\right)^{1/2}$

[a]Data taken from Shih et al. 2005.

In the field, the methods of determining ε include measuring the velocity strains directly from vertical profiling instruments, determining the velocity spectrum from time series at a fixed point, and measuring the temperature gradient spectrum (e.g., Gregg 1999, Prandke 2005). The turbulent length scale l is usually not reported; rather it is implicitly assumed that Re_T is large. There are many issues with regard to processing these data; for example, all nine components of the dissipation tensor ε are not measured, and one must resort to assumptions regarding isotropy to infer the value of the unknown components (e.g., Itsweire et al. 1993, Stips 2005). However, the main problems are probably not in estimation, but rather in interpretation as either one or both of the nondimensional ratios in Equation 2b are likely not zero. This unsteadiness and patchiness have led to debate over sampling and interpretation (e.g., Baker & Gibson 1987, Baumert et al. 2005, Davis 1996), and hence the applicability of the dynamical models in Equations 5 and 9. For example, in a recent experiment in a lake thermocline, Etemad-Shahidi & Imberger (2006) found the turbulence was both highly intermittent and patchy, with an average of only 30% of the thermocline actively turbulent, and simple arithmetic averaging indicated that the overall vertical turbulent transport was close to the molecular limit.

Researchers have made direct measurements of vertical mixing in both the ocean and in lakes using dye–tracer release experiments, and Wuest & Lorke (2005) examined these field experiments in a recent review. The dye-tracer experiments involved the injection of a known mass of a passive tracer, such as sulfur hexafluoride or uranin, mapping the subsequent time development of the three-dimensional spreading tracer cloud, horizontally averaging the data, and finally solving a simple one-dimensional vertical turbulent diffusion equation to find the unknown (constant) vertical tracer diffusivity K_Z. In some cases, turbulent microstructure measurements have also been made during the tracer release to compute a single vertical diffusivity K_ρ. There are significant difficulties with each method. For example, if the tracer reaches the boundaries, the tracer concentration is no longer described by simple one-dimensional vertical transport. In the case of the microstructure, it seems highly unlikely that all the assumptions required to use either Equation 5 or 9 are satisfied in the field. If the dynamical assumptions are not true for one cast, how does averaging over many casts improve the estimates? How does one weigh the relatively high values of dissipation typically seen in the boundary layer with the low values seen in the interior to assess a basinwide average? It seems reasonable to reflect on whether these questions can be answered in the absence of a statistical model of the spatial, temporal, and dynamical character of the mixing events themselves. Nevertheless, Wuest & Lorke (2005) conclude in their review that the tracer and turbulence measurements (using a constant $\Gamma \approx 0.2$) are remarkably consistent, usually to within a factor of 2 or 3.

The results also show how the diffusivity and the turbulence intensity parameter $\varepsilon/\nu N^2$ vary spatially in both lakes and the ocean. For example, the diffusivity in the interior of lakes is as low as $O(\kappa)$, whereas in the interior of the oceans it is typically of $O(10^2\kappa)$. However, as one approaches the bottom, the diffusivities increase and reach values up to $O(10^2\kappa)$ in lakes and $O(10^4\kappa)$ in the oceans. Furthermore, the values of $\varepsilon/\nu N^2$ also vary strongly, from as little as $O(1)$ in the thermocline (e.g., Wuest & Lorke 2005) to as high as $O(10^5)$ in parts of the deep ocean (e.g., Ferron et al. 1998).

Given this variability, and the existence of such extremes, how can we reconcile using a constant $\Gamma \approx 0.2$ in our parameterizations of the fluxes?

Both laboratory and DNS work indicate that at these extremes, when either $\varepsilon/\nu N^2 \sim O(1)$ or $\varepsilon/\nu N^2 \sim O(10^5)$, the mixing efficiency $R_f \to 0$ and the use of large $R_f \approx 0.2$ in field situations in these limits cannot be justified. This is not simply a matter of curiosity. There is a fundamental inconsistency between the results from the laboratory and DNS experiments and the inference of diffusivity from microstructure in the field that remains unresolved.

From a global perspective, this inconsistency needs to be resolved. Observations show that the oceans are not uniformly and steadily agitated, but rather there is a relatively quiescent interior and turbulent hot spots, often near boundaries. This paradigm is central to global-scale ocean dynamics (e.g., Wunsch & Ferrari 2004), and researchers are increasingly focusing their attention on potential hot-spot regions. Two issues are important here. First, the geography of mixing hot spots and the dynamics responsible for their spatial and temporal distribution need to be determined. Second, the fundamental inconsistency between present practice and theoretical and experimental evidence needs to be reconciled. Progress on both fronts is required if we are to scale up local information to assess basin-scale influences with any confidence. For example, the mixing efficiency R_f in energetic boundary regions is needed even to close simple energy budget models (e.g., Munk & Wunsch 1998, Wunsch & Ferrari 2004), and there is a big difference between the model predictions if one uses an efficiency of either 0.2 or 0.02.

Mixing in the Interior of the Ocean

In the stratified interior of natural water bodies, we distinguish a second class of mixing problems that are characteristically intermittent, typically occurring within turbulent patches that grow and decay with time. These patches are not driven directly by boundary stresses or instabilities of the ambient flow, but rather they result from the transport of energy by internal gravity waves and, in particular, by the disruption of that transport through scale-transforming interactions between either waves of different scales or between waves and ambient flows (e.g., Carter & Gregg 2006, Garrett 2003).

For these events, the length scale ratio l/L is an indicator of the importance of patch boundary dynamics, i.e., the dynamics and hence fluxes occurring in the transition regions separating active turbulent flow from the laminar, stratified exterior flow. In the limit $l/L \to 0$, patch boundary processes are negligible, and the spatially homogeneous scaling discussed above may be appropriate. For finite values of l/L, however, patch boundary processes are fundamentally important and may in fact be the rate-controlling process determining the overall scalar flux produced by an individual event. A steady-state situation can only exist if the vertical turbulent flux in the patch interior matches the flux at the patch boundaries; otherwise the resulting vertical flux divergence causes a local change in the density distribution with time. If the flow is unsteady, fluxes in the patch interior cannot be simply related to the fluxes of fundamental interest in the patch transition zones.

This simple example illustrates our present conundrum. We wish to infer the fluxes linking isolated mixing events to a global scalar distribution, but the primary tool for inferring fluxes from observations is currently based on a theory that explicitly neglects both the existence of the transition regions separating turbulent from nonturbulent regions and the processes that determine fluxes in these regions. It is precisely through these patch boundary fluxes, currently not accounted for appropriately, that isolated turbulent mixing events can influence the larger-scale transport and distribution of scalar quantities.

Decades of observations in the ocean thermocline and in lakes suggest that two defining characteristics of turbulence in these environments are its patchiness in space and its intermittency in time, both of which suggest turbulent events triggered by dynamical instabilities and therefore regimes characterized by the growth and decay of turbulent intensity. Arguably, observations are never obtained from a quasi-steady-state regime, so even if one were to accept a universal mixing efficiency of 0.2, there is no compelling reason to assume that inferred fluxes in an isolated patch interior can be meaningfully related to the communicative fluxes between the patch and its ambient environment.

DNS of isolated mixing events such as those produced by shear instabilities and breaking internal waves supports these arguments. Although necessarily idealized, these types of simulations show that carefully measured diapycnal fluxes (e.g., Winters & D'Asaro 1996) evolve through growth and decay phases, often with no significant steady or nearly steady regime. Furthermore, the spatial locations of high dissipation rates tend to occur in the patch interiors, whereas the locations of maximum scalar fluxes are often at the patch boundaries, although the degree of this separation varies considerably with the evolutionary stage of the event. Furthermore, there is an indication that the preturbulent phase of some instabilities can produce significant straining and diffusive flux in the absence of significant dissipation, leading to some dependence of the mixing efficiency on time and Pr during the initial phase of an instability, but not on Re_T once this exceeds a threshold level (e.g., Smyth et al. 2001). As always, caution is required when interpreting such experiments in a field or geophysical context. Nevertheless, these types of simulations reveal clearly the importance of fluxes at patch boundaries and the degree to which temporal evolution invalidates the assumption that instantaneous dissipation rates in patch interiors are easily related to mixing rates.

Mixing in the stratified interior of the ocean requires energy and, in the context of this discussion, a remote source of internal waves. Particularly energetic waves are topographically excited at the M_2 tidal frequency and at near-inertial frequencies owing to surface wind forcing. Once generated, these waves propagate into the stratified interior. The dynamics and fate of radiating internal waves in natural water bodies are the subject of a large body of research, well beyond the scope of this review (e.g., see Alford 2003, Garrett & Kunze 2007). Nevertheless, the dynamic evolution of the radiating wave field is intimately connected to mixing in the stratified interior. For the purposes of our discussion here, there are two fates of interest for radiating internal wave energy. First, energy may radiate from generation sites to a remote boundary at which it is lost to dissipation and mixing via processes such as critical reflection. A

second possibility is that wave nonlinearities alter the wave field such that, within the stratified interior, energy is transferred to small scales in which dynamical instabilities occur, leading to localized dissipation and mixing.

This second scenario is not equally likely at all spatial locations because wave generation and therefore radiative fluxes vary spatially and temporally owing to a dependence on topography, ambient flows, and atmospheric conditions. An oft-cited example comes from the Brazil Basin (Polzin et al. 1997), where researchers observed significantly elevated dissipation rates in the eastern portion of the basin above rough topography compared with the much lower values found above the smooth bathymetry in the western basin. The elevated dissipation rates extend to a few kilometers above the bottom, implying that the dissipation and mixing are sustained by upwardly radiating internal gravity waves.

Numerical simulations of upward propagating waves, with scales and intensity chosen to match the Brazil Basin observations as closely as possible, revealed that such waves are susceptible to a parametric subharmonic instability that rapidly transfers energy from the directly forced waves to highly sheared near-inertial motions of small vertical scale (MacKinnon & Winters 2003). A simple scaling argument combining the vertical group velocity of the forced waves with the numerically observed rate at which energy is transferred to small scales yields an estimate of the characteristic vertical scale of the region over which wave-driven mixing can be supported by this mechanism. The numerical simulations show reasonable agreement with the observations both in terms of the magnitude and vertical decay scale of the wave-driven mixing.

The mechanism by which energy is extracted from the upwardly radiating waves is only operative in latitudes less than 28.9° for which half the M_2 tidal frequency is greater than the local inertial frequency (MacKinnon & Winters 2005). Simulations of identically forced waves at higher latitudes propagate freely through the water column without contributing energy for mixing. These observations, together with the hypothesized wave dynamics suggested by simulation, suggest that even within the stratified interior of the ocean, there are likely hot spots of significantly elevated mixing. The geography of these hot spots is likely to be sensitive not only to locations of topographic forcing and to variable flow conditions at the generation sites, but also to latitude (see **Figures 3** and **4**).

A second example involves the radiating internal tide from the Hawaiian Ridge. Researchers have modeled internal tides and observed them propagating away from the ridge in the form of low vertical modes along beamlike trajectories extending into the Pacific basin. The energy for these waves is extracted from barotropic tidal currents and converted into radiating internal gravity waves as the flow is deflected vertically in the vicinity of the ridge. Although estimates are not precise, it is currently believed that the majority of the energy extracted from the barotropic tide is radiated away from the ridge as waves, whereas a much smaller fraction is dissipated locally in the topographic boundary layer. Where this radiating energy dissipates is an open question. Unless it is able to propagate across the entire basin to the continental slope and shelf, it appears that this energy must dissipate somewhere in the stratified interior of the deep ocean. As in the first example, idealized numerical studies have

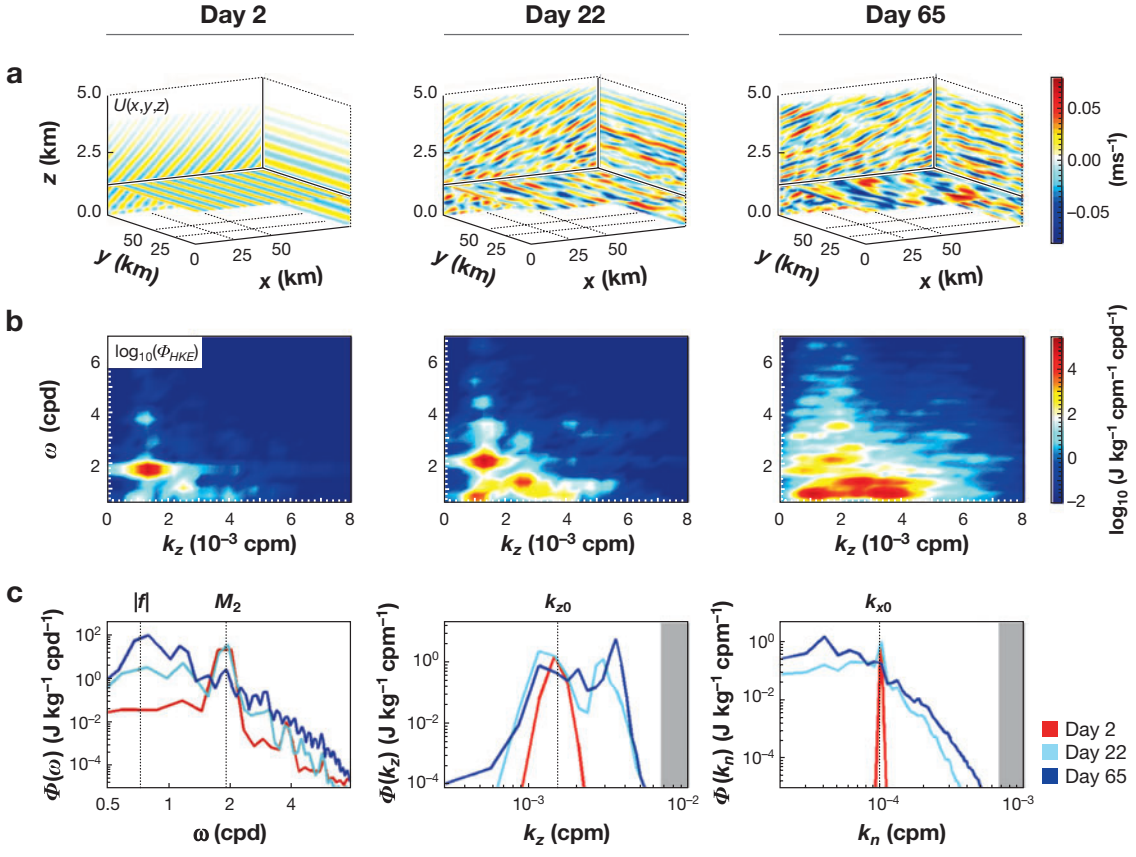

Figure 3

Snapshots at three times during the evolution of an upward propagating internal tide at 21 S. (*a*) Eastward horizontal velocity. (*b*) Spectral (horizontal kinetic) energy density as a function of vertical wave number and frequency, calculated from 4-day time series surrounding the times of each snapshot in the top panels. (*c*) Power spectra for each time period as a function of frequency (*left*), vertical wave number (*middle*), and horizontal wave number (*right*): day 2 (*red line*), day 22 (*light blue line*), and day 65 (*dark blue line*). Parametric subharmonic instability transfers energy from the bottom forced wave at M_2 to nearly horizontal motions at smaller vertical scale. A scale-selective dissipation operator acts to dissipate energy at the smallest resolved scales, and, assuming that energy transferred to these scales is ultimately balanced by local dissipation, the rate of energy transfer to small scales is interpreted as the wave-driven dissipation rate. Figure taken from MacKinnon & Winters 2007.

suggested that wave instabilities related to parametric subharmonic instability at the critical latitude of 28.9° (at which the subharmonic 0.5 M_2 matches the local inertial frequency f) may play a role (MacKinnon & Winters 2003; J.A. MacKinnon & K.B. Winters, submitted).

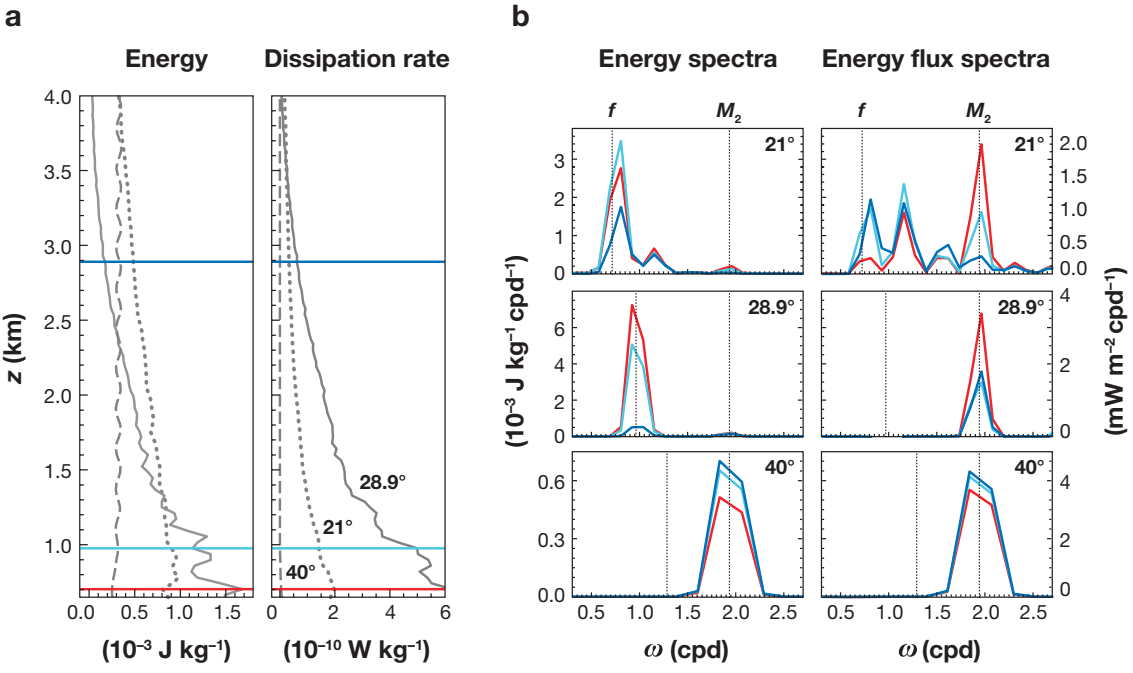

Figure 4

(*a*) Steady-state average vertical structure of energy (kinetic plus potential) and dissipation rate for simulations at 21°, 28.9°, and 40°. The horizontal colored lines indicate the depths of spectra shown in the columns at right. (*b*, *left column*) Energy spectra for each latitude at three representative depths. The M_2 tidal frequency and the local inertial frequency are indicated with vertical lines. (*b*, *right column*) Energy flux spectra for each latitude at three representative depths. Note the change in axis range. Energy spectra at all depths show peaks at the tidal frequency and two near-subharmonic frequencies, although almost all the energy accumulates at the lower, near-inertial frequency. Near the bottom, energy flux is primarily tidal but shifts progressively to subharmonic waves with increasing height. Integrated over all frequencies, the upward energy flux steadily declines with increasing height above the bottom. In steady state, this flux convergence is balanced by turbulent dissipation. Figure taken from MacKinnon & Winters 2007.

CONCLUSIONS

The present methodology for estimating vertical mixing in geophysical environments utilizes indirect inferences from vertical profiles of either the rate of dissipation of turbulent kinetic energy or, less commonly, the rate of dissipation of temperature variance. The theoretical framework supporting these inferences was advanced in 1972 and 1980. As practiced today, there are three fundamental problems with our current practices.

Firstly, even in steady, homogeneous regimes, the mixing efficiency is not constant but depends on the fundamental dimensionless parameters describing turbulent, stratified shear flows. Evidence that the mixing efficiency is not a universal constant

has been in the literature for decades. Secondly, the framework itself is intrinsically inapplicable when turbulent mixing occurs in spatially localized intermittent patches. At least two additional dimensionless parameters are required to account for this additional complexity. Thirdly, sampling problems remain a first-order issue in geophysical settings. The geography of mixing events is not well understood, although there are strong indications that it depends on proximity to topographic, atmospheric forcing and latitude. There is little theoretical justification for treating an ensemble of observations from dynamical regimes characterized by spatial locality and temporal evolution as if they were obtained from a spatially homogeneous, steady flow.

The current thinking suggests that mixing in the interior of the ocean and lakes is negligible when compared with that accomplished in the turbulent boundary layers. Although this may be true to a degree, we suggest it may be premature to abandon the interior mixing problem. At least in the ocean, there are clearly identifiable energy sources for sustaining turbulent fluxes: winds and tides/topography. Evidence that this energy is dissipated exclusively at the boundaries has not been established. Evidence that this energy is not dissipated in the stratified interior is indirect. Unfortunately, decades of ship-based measurements of dissipation rates of turbulent kinetic energy do not begin to approach a reliable sampling of the overall turbulent structure of the ocean interior. Tracer release studies are potentially attractive because they can provide a temporally integrated view of the fluxes associated with multiple individual events in a region. To date, however, relatively few studies have been carried out, and the technique is probably too prohibitively expensive to be considered for large-scale spatial surveys.

DISCLOSURE STATEMENT

The authors are not aware of any biases that might be perceived as affecting the objectivity of this review.

ACKNOWLEDGMENTS

G.N.I. was supported by the Australian Research Council, K.B.W. was supported by National Science Foundation Grant No. OCE-0425283 and Office of Naval Research Grant No. N00014-05-1-0573, and J.R.K. was supported by Office of Naval Research Grant Nos. N00014-13-1-0422 and N00014-92-J-161.

LITERATURE CITED

Alford MH. 2003. Redistribution of the energy available for ocean mixing by long-range propagation of internal waves. *Nature* 423:159–62

Baker MA, Gibson CH. 1987. Sampling turbulence in the stratified ocean: statistical consequences of strong intermittency. *J. Phys. Oceanogr.* 17:1817–36

Barry ME, Ivey GN, Winters KB, Imberger J. 2001. Measurements of diapycnal diffusivity in stratified fluids. *J. Fluid Mech.* 442:267–91

Baumert HZ, Simpson J, Sundermann J, eds. 2005. *Marine Turbulence: Theories, Observations and Models*. Cambridge, UK: Cambridge Univ. Press
Briggs DA, Ferziger JH, Koseff JR, Monismith SG. 1998. Turbulent mixing in a shear-free stably stratified two-layer fluid. *J. Fluid Mech.* 354:175–208
Carter GS, Gregg MC. 2006. Persistent near-diurnal internal waves observed above a site of M2 barotropic-to-baroclinic conversion. *J. Phys. Oceanogr.* 36:1136–47
Davis RE. 1996. Sampling turbulent dissipation. *J. Phys. Oceanogr.* 26:341–58
Durski SM, Glenn SM, Haidvogel DB. 2004. Vertical mixing schemes in the coastal ocean: comparison of the level 2.5 Mellor-Yamada scheme with an enhanced version of the K profile parameterization. *J. Geophys. Res.* 109:1–23
Etemad-Shahidi A, Imberger J. 2006. Diapycnal mixing in the thermocline of lakes: estimations by different methods. *Environ. Fluid. Mech.* 6:227–40
Ferron B, Mercier H, Speer K, Gargett A, Polzin K. 1998. Mixing in the Romanche Fracture Zone. *J. Phys. Oceanogr.* 28:1929–45
Garrett C. 2003. Oceanography: mixing with latitude. *Nature* 422:477–79
Garrett C, Kunze E. 2007. Internal tide generation in the deep ocean. *Annu. Rev. Fluid Mech.* 39:57–87
Gregg MC. 1999. Uncertainties and limitations in measuring ε and χ. *J. Atmos. Ocean. Technol.* 16:1483–90
Itsweire EC, Helland KN, Van Atta CW. 1986. The evolution of grid-generated turbulence. *J. Fluid Mech.* 162:299–338
Itsweire EC, Koseff JR, Briggs DA, Ferziger JH. 1993. Turbulence in stratified shear flows: implications for interpreting shear-induced mixing in the ocean. *J. Phys. Oceanogr.* 23:1508–22
Ivey GN, Imberger J. 1991. On the nature of turbulence in a stratified fluid, part 1: the energetics of mixing. *J. Phys. Oceanogr.* 21:650–58
Jackson P, Rehmann CR. 2003. Laboratory measurements of differential diffusion in a diffusively stable, turbulent flow. *J. Phys. Oceanogr.* 33:1592–603
Keller K, Van Atta CW. 2000. An experimental investigation of the vertical temperature structure of homogeneous stratified shear turbulence. *J. Fluid Mech.* 425:1–29
Lemckert CJ, Antenucci JP, Saggio A, Imberger J. 2004. Physical properties of turbulent benthic boundary layers generated by internal waves. *J. Hydraul. Eng.* 130:58–69
Linden PF. 1979. Mixing in stratified fluids. *Geophys. Astrophys. Fluid Dyn.* 13:3–23
MacKinnon JA, Winters KB. 2003. Spectral evolution of bottom-forced internal waves. *Near-Bound. Process. Parameterization, Proc. 13th 'Aha Huliko'a Hawaii. Winter Workshop*, pp. 73–83. Honolulu: School Ocean Earth Sci. Technol.
MacKinnon JA, Winters KB. 2005. Subtropical catastrophe: significant loss of low-mode tidal energy at 28.9. *Geophys. Res. Lett.* 32:1029–33
Munk W, Wunsch C. 1998. Abyssal recipes II, energetics of tidal wind motion. *Deep-Sea Res. Part 1* 45:1977–2010
Oakey NS. 1982. Determination of the rate of dissipation of turbulent energy from simultaneous temperature and velocity shear microstructure measurements. *J. Phys. Oceanogr.* 12:256–71

Osborn TR. 1980. Estimates of the local rate of vertical diffusion from dissipation measurements. *J. Phys. Oceanogr.* 10:83–89
Osborn TR, Cox CA. 1972. Oceanic fine structure. *Geophys. Fluid Dyn.* 3:321–45
Prandke H. 2005. Microstructure sensors. See Baumert et al. 2005, pp. 101–9
Riley JJ, Lelong M-P. 2000. Fluid motions in the presence of strong, stable stratification. *Annu. Rev. Fluid Mech.* 32:613–57
Polzin KL, Toole JM, Ledwell JR, Schmitt RW. 1997. Spatial variability of turbulent mixing in the abyssal ocean. *Science* 276:93–96
Rohr JJ, Itsweire EC, Helland KN, Van Atta CW. 1988. Growth and decay of turbulence in a stably stratified shear flow. *J. Fluid Mech.* 195:77–111
Rohr JJ, Itsweire EC, Van Atta CW. 1984. Mixing efficiency in stably-stratified decaying turbulence. *Geophys. Astrophys. Fluid Dyn.* 29:221–36
Saggio A, Imberger J. 2001. Mixing and turbulent fluxes in the metalimnion of a stratified lake. *Limnol. Oceanogr.* 46:392–409
Sherman JT, Davis RE. 1995. Observations of temperature microstructure during NATRE. *J. Phys. Oceanogr.* 25:1913–29
Shih LH, Koseff JR, Ivey GN, Ferziger JH. 2005. Parameterization of turbulent fluxes and scales using homogenous sheared stably stratified turbulence simulations. *J. Fluid Mech.* 525:193–214
Smyth WD, Moum JM, Caldwell DR. 2001. The efficiency of mixing in turbulent patches: inferences from direct simulations and microstructure observations. *J. Phys. Oceanogr.* 31:1969–92
Stacey MT, Monismith SG, Burau JR. 1999. Observations of turbulence in a partially stratified estuary. *J. Phys. Oceanogr.* 29:1950–70
Staquet C, Sommeria J. 2002. Internal gravity waves: from instability to turbulence. *Annu. Rev. Fluid Mech.* 34:559–93
Stillinger DC, Helland KN, Van Atta CW. 1983. Experiments on the transition of homogeneous turbulence to internal waves in a stratified fluid. *J. Fluid Mech.* 131:91–122
Stips A. 2005. Dissipation measurement: theory. See Baumert et al. 2005, pp. 115–26
Troy CD, Hult EL, Koseff J. 2006. Experiments on a strongly-stratified turbulent patch with periodic forcing. *Proc. 6th Int. Symp. Strat. Flows*, pp. 410–15. Perth, Aust.: School Environ. Syst. Eng.
Winters KB, D'Asaro EA. 1996. Diascalar flux and the rate of fluid mixing. *J. Fluid Mech.* 317:179–93
Wuest A, Lorke A. 2005. Validation of microstructure-based diffusivity estimates using tracers in lakes and oceans. See Baumert et al. 2005, pp. 139–52
Wunsch C, Ferrari R. 2004. Vertical mixing, energy, and the general circulation of the oceans. *Annu. Rev. Fluid Mech.* 36:281–314

Annual Review of
Fluid Mechanics

Volume 40, 2008

Contents

Indexes

Errata

An online log of corrections to *Annual Review of Fluid Mechanics* articles may be found at http://fluid.annualreviews.org/errata.shtml